

Theme Issue Article

Shiga toxins, glycosphingolipid diversity, and endothelial cell injury

Johannes Müthing¹; Christian H. Schweppe^{1,2}; Helge Karch^{1,2}; Alexander W. Friedrich^{1,2}¹Institute for Hygiene, University Hospital Münster, Münster, Germany; ²Interdisciplinary Center for Clinical Research, Münster, Germany

Summary

Shiga toxin (Stx)-producing *Escherichia coli* (STEC) cause an enteric illness that results in a spectrum of outcomes ranging from asymptomatic carriage to uncomplicated diarrhea, bloody diarrhea, and the postdiarrheal haemolytic uremic syndrome (HUS), which leads to renal and other organ microvascular thrombosis. Binding of Stx to the glycosphingolipid (GSL) globotriaosylceramide (Gb3Cer/CD77) on endothelial cells followed by receptor-mediated endocytosis is the linchpin in STEC-mediated disease. Only GSLs that associate strongly with lipid rafts appear to carry Stxs retrogradely from the plasma membrane through the Golgi apparatus to the endoplasmic reticulum where they are translocated to the cytosol and exert their toxic function. Thus, the biophysical features of the lipid moiety of GSL receptors may influence its incorporation into certain membrane domains and thereby affect toxin destination. Consequently, a de-

tailed structural analysis of Stx-binding GSLs is required to illuminate the molecular causes that may underlie the different Stx susceptibilities of endothelial cells derived from various vascular beds. Solid phase overlay binding assays of thin-layer chromatography (TLC)-separated GSL preparations employing specific antibodies and/or Stxs in conjunction with anti-Stx-antibodies are commonly used for the identification of Stx-binding GSLs. Such GSL-profiling combined with matrix-assisted laser desorption/ionization time-of-flight mass spectrometry (MALDI-TOF-MS) represents a convenient strategy to structurally characterize Stx-receptors from any biological sources such as primary cells, cell lines, or organs. This approach may be helpful to gain insights into Stx-induced impairment of target cells that is suggested to originate at least partly from the structural heterogeneity of the cellular ligands of Stxs.

Keywords

STEC, Gb3Cer, endothelial cells, TLC overlay assay, MALDI-TOF-MS

Thromb Haemost 2009; 101: 252–264

Shiga toxins and their association with clinical outcome of human infections

Shiga toxin (Stx)-producing *Escherichia coli* (STEC), especially of serotype O157:H7, cause a food- or waterborne enteric illness that results in a spectrum of outcomes ranging from asymptomatic carriage to uncomplicated diarrhea, bloody diarrhea, and the haemolytic uremic syndrome (HUS), a leading cause of acute renal failure in children (1–3). After ingestion, Stxs are released by STEC in the intestine, translocated across the gut epithelium into the circulation, and transported to capillary endothelial cells in renal glomeruli and other organs. Host cells are then injured by inhibiting the protein synthesis, stimulating prothrombotic messages, or inducing apoptosis. Vascular injury during HUS re-

sults from the action of Stxs on vascular endothelial cells (3, 4). The net result is a multi-organ thrombotic process (4).

Stxs are presently the most important and best characterized STEC virulence factors that can cause microvascular endothelial injury. They are AB₅ ribosome-inactivating toxins with rRNA-*N*-glycosidase activity (5, 6). Based on cell-culture toxin-neutralization assays and nucleotide sequence analysis, Stxs can be divided into two major groups, Stx1 and Stx2 (7). The prototype toxins of these families display 57% and 60% nucleotide sequence identity in their A and B subunits, respectively (8). Each of the Stx groups contains an increasing number of variants (Table 1). A single strain can possess one or more different *stx* alleles (9–14) and the different *stx* subtypes are associated with different clinical outcomes of infections (9–11, 14–17) (Table 1). The Stx1 group includes, in addition to the prototype Stx1, two

Correspondence to:
Prof. Dr. Johannes Müthing
Institut für Hygiene, Universitätsklinikum Münster
Robert-Koch-Str. 41, 48149 Münster, Germany
Tel.: +49 251 83 55192, Fax: +49 251 83 55341
E-mail: jm@uni-muenster.de

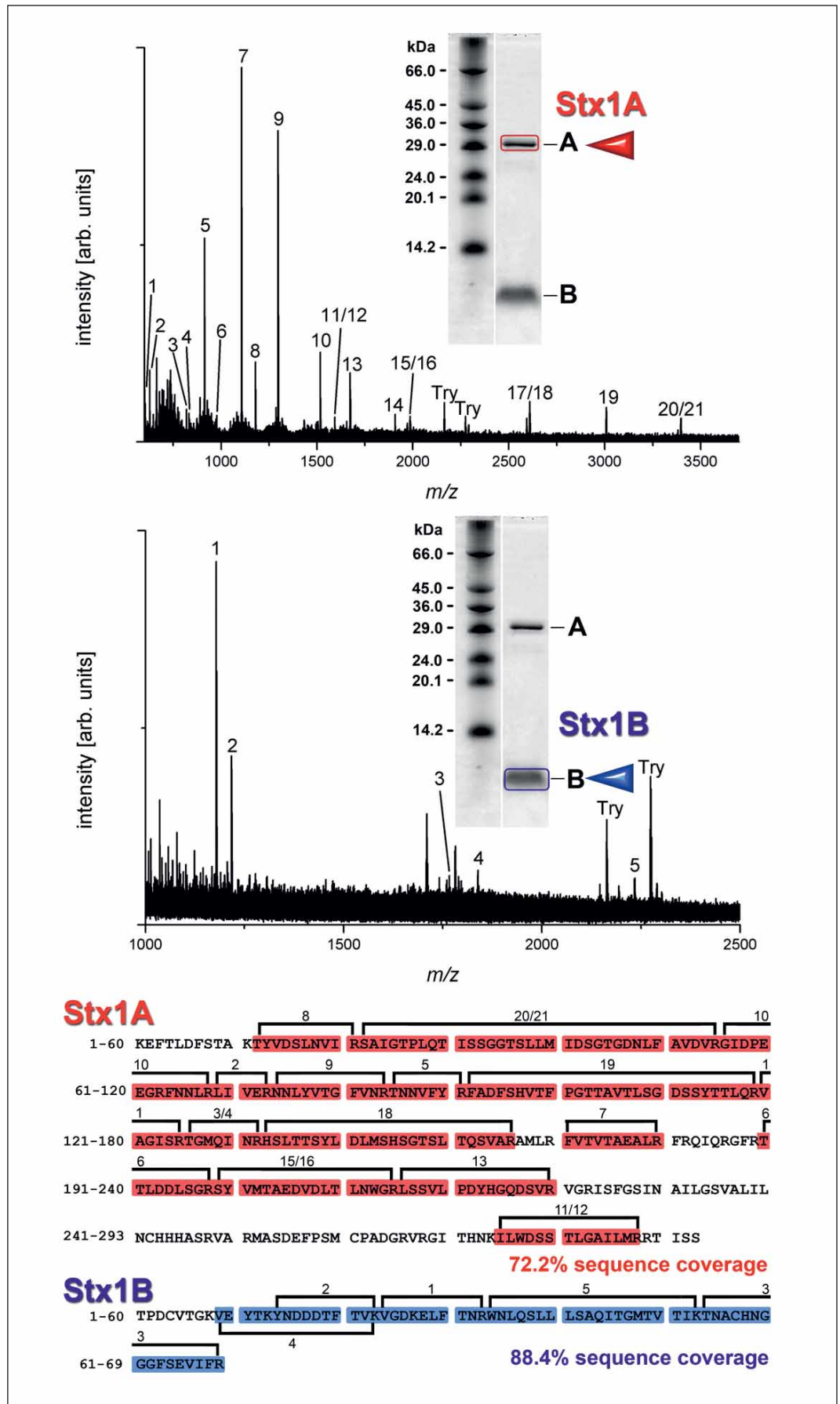
Financial support:
We are thankful for continuous support of our work by grants from the Deutsche Forschungsgemeinschaft (DFG), SPP 1130 project KA 717/4–2 (H.K.), SFB 293 project A18 (H.K.), the cooperative projects FR2569/1–1 (A.W.F.) and MU845/4–1 (J.M.), the GRK 1409/1 and grants from the Interdisciplinary Center of Clinical Research (IZKF) Münster, project no. Ka2/061/04 (H.K.) and Me2/023/08 (A.M.)

Received: May 23, 2008
Accepted after minor revision: July 9, 2008

Prepublished online: January 15, 2009
doi:10.1160/TH08-05-0317

Figure 1: Peptide maps of tryptic in-gel-digested A and B subunits of StxI and structural assignment.

Three µg of purified StxI together with 20 µg of reference proteins were applied to SDS-PAGE under reducing conditions and stained with Coomassie blue. Separated StxIA and StxIB were digested in gel with trypsin and the resulting peptide mixture subjected to MALDI-TOF-MS according to Shevchenko et al. (62) and a protocol previously published (171). All experimentally derived *m/z*-values of peaks 1 to 21 of StxIA and peaks 1 to 5 of StxIB were submitted to ProteinProspector (UCSF Proteomic tools, v4.27.2) and ALDENTE (Peptide Mass Fingerprinting tool available at the ExPASy proteomics server from the SWISS Institute of Bioinformatics SIB). StxIA and StxIB unrelated fragment ions caused by autoproteolytic digestion of trypsin are labeled with "Try" in the spectra. The ions with low mass (*m/z* between 1000 and 1250) in the StxIB peptide map represent detergent-derived impurities of the peptide preparation. The peptide mass search resulted in the identification of StxIA (Shiga-like toxin I subunit A precursor; EC 3.2.2.22, rRNA *N*-glycosidase) encoded by the bacteriophage HI9 composed of 315 amino acids with a molecular mass of 34,814 Da (accession number: P08026; excluding the signaling peptide: 293 amino acids, 32,398 Da) and StxIB (Shiga-like toxin I subunit B) composed of 89 amino acids with a molecular mass of 9,743 Da (accession number: P69179, excluding the signaling peptide: 69 amino acids, 7,691 Da), both from *E. coli*. Those data fit well to the apparent molecular masses of ~32 kDa and ~7.7 kDa determined by SDS-PAGE for the A and B subunit, respectively. The database comparison of the submitted list of tryptic peptides resulted in a sequence coverage of 72.2% for StxIA (highlighted in red) and 88.4% for StxIB (highlighted in blue).



variants designated Stx1c (10, 18) and Stx1d (19, 20), which are frequently found in STEC isolated from patients with uncomplicated diarrhea (9, 10, 13, 14, 18). The Stx2 family is comparably more heterogeneous. Besides the classical Stx2, it comprises several variants of which Stx2c (21), Stx2c2 (22), Stx2d (23), the mucus-activatable Stx2d (Stx2d_{activatable}) (24), Stx2e (25), and Stx2f (26–28) were identified in STEC isolated from patients (Table 1). Stx2, Stx2c, and Stx2d_{activatable} are associated with severe human disease such as HUS and bloody diarrhea (9, 11, 13–15, 17, 29). The remaining Stx2 variants have been mostly identified in STEC isolated from patients with uncomplicated diarrhea or from asymptomatic shedders (9, 10, 14, 18, 23, 25), but are rarely found in HUS patients (14, 30). Stx2e, the major Stx type associated with the edema disease in swine, is rare in human STEC (9, 13, 14, 25). Stx2f is a common Stx variant expressed by STEC isolated from pigeons (31). Its presence in human STEC isolates is the exception (9, 13, 14, 26–28, 32). However, from recent studies focusing on the *stx* genes it becomes obvious that several *E. coli* strains represent a highly dynamic system during the course of human infection that can modulate the pathogens in both directions due to the loss or gain of *stx*-converting bacteriophages (33–37).

Biochemical features and mode of action of AB₅ Stxs

All members of the Stx family are composed of a single enzymic ~32 kDa A subunit (38) non-covalently associated with five ~7.7 kDa B subunits. The pentameric B subunit, which may contain as many as 15 binding sites for its preferential glycosphingolipid (GSL) receptor globotriaosylceramide (Gb3Cer) (39), mediates attachment and internalization of the AB₅-Gb3Cer complex by receptor-mediated endocytosis via clathrin-coated vesicles (7, 40) or by endocytic routes that do not involve clathrin-coated pits ([41–43] and references therein).

In Stx-sensitive cells the toxin-receptor complex undergoes retrograde transport from early endosomes through the cisternae of the *trans*-Golgi network to the endoplasmic reticulum (ER) and even to the nuclear membrane (44–46). Once Stx has reached the ER, the ~32 kDa A subunit is cleaved by the membrane-anchored protease furin into a catalytically active ~27.5 kDa A₁ and a ~4.5 kDa A₂ fragment. This processing is required for retro-translocation into the cytosol, where the A₁ subunit exerts its rRNA *N*-glycosidase activity that removes a specific adenine residue from 28S rRNA (47). The proteolytic cleavage is essential for maximal cytotoxicity of Stx1 from *E. coli* O157:H7 (48), and about one molecule of translocated A₁ fragment of Stx1 per cell is sufficient to inhibit protein synthesis and kill a cell (49).

It has been known for some time that following the intracellular routing of Stxs to the nuclear membrane Stxs trigger programmed cell death signalling cascades in intoxicated cells (6, 50, 51). This is important because for unknown reasons a variety of cells succumb to apoptotic cell death rather than to necrosis through inhibition of cytoplasmic protein synthesis. The mechanisms of apoptosis induction are newly emerging and suggest that Stx-induced apoptosis may contribute to the pathogenesis of HUS caused by STEC (4, 52, 53). Furthermore, Stx causes

sublethal cell injury by altering cell adhesive properties and by increasing endothelial susceptibility to leukocyte-mediated injury (54). The resulting injured endothelium changes its normal thromboresistant phenotype and becomes thrombogenic, initiating microvascular thrombus formation (55, 56).

Stx purification and structural assignments to A and B subunits

Facile methods for affinity chromatography purifying Stxs are based on their binding specificity using immobilized truncated synthetic analogs of the receptor (57), Gb3Cer-conjugated octyl Sepharose CL-4B (58) or Gb3Cer non-covalently immobilized onto silica gel (59). However, conventional purification procedures of Stxs employing ammonium sulfate precipitation, followed by Sephacryl S200 and Affi-Gel Blue column chromatography, chromatofocussing and high-performance liquid chromatography are still as relevant and useful (60, 61). In addition to a preliminary proof of the apparent purity and structural integrity of a purified toxin by SDS-PAGE, peptide-mass mapping performed by matrix-assisted laser desorption ionization time-of-flight mass spectrometry (MALDI-TOF-MS) of tryptic peptides obtained from in-gel digests represents one of the most commonly employed approaches to rapidly identify proteins from a gel band or gel spot (62, 63). The structural verification of SDS-PAGE-separated Stxs following their purification according to standard procedures (60, 61) is fast and convenient, and it requires only a few micrograms of toxins. The resulting peptide maps of the A and B subunits of Stx1 and Stx2 are shown in Figures 1 and 2 together with the corresponding Coomassie blue-stained bands and the amino acid sequence coverages. The peptide mass search in sequence databases allows the identification of the A and B subunits of both toxins thereby confirming Stx1 and Stx2 as the “unknown” proteins in accordance with high sequence coverages of the subunits of the toxins (for details see figure legends). In addition, the amino acid sequence alignments of the matched peptide fragments illustrate the rather low degree of homology of the A and B subunits of the two closely related members of the Stx family (8, 64). Such control of purity and precise biochemical structure is highly recommended as a first step for the characterization of any Stx-preparation for physiological or receptor binding assays.

Cellular ligands of Stxs

GSLs are components of all vertebrate cells and distribute with high specificity between mammalian species, organs (65, 66), and cell types (67, 68). GSLs are known to play a fundamental role during development and cell differentiation (69, 70) and to mediate a wide variety of cellular processes, including cellular growth (71), signal transduction (72), and cell-cell interaction (73).

GSLs are amphipathic molecules composed of a hydrophilic carbohydrate chain and a hydrophobic ceramide anchor (74, 75). In mammalian cells, the ceramide moiety is typically generated from the long-chain aminoalcohol sphingosine (d18:1), which is linked with a fatty acid varying in chain length from C16 to C24.

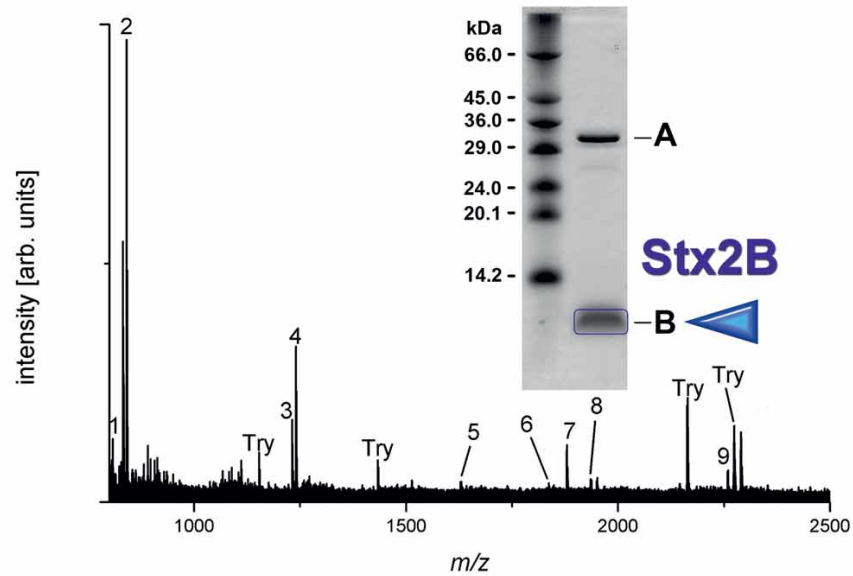
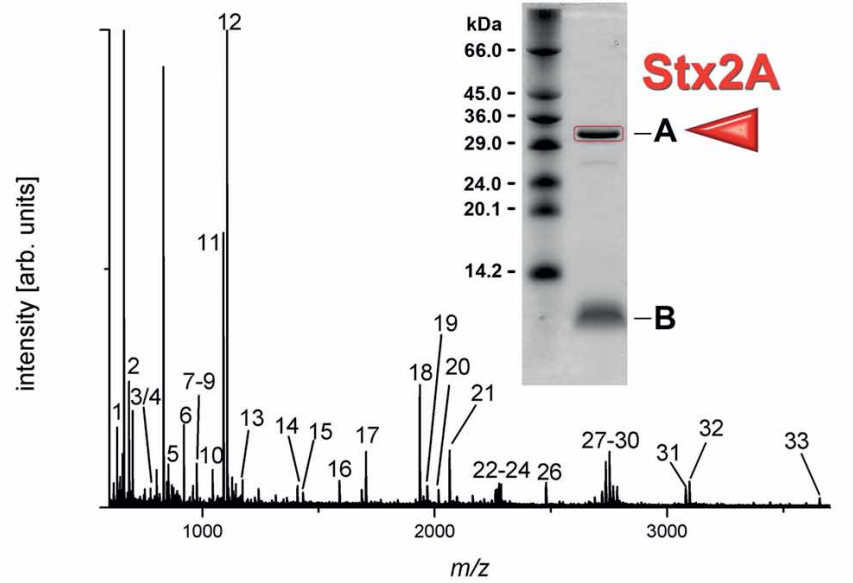
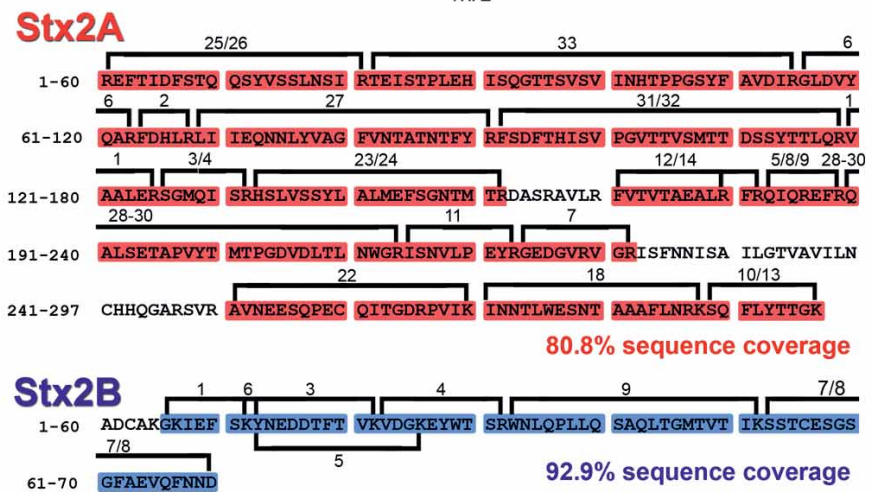


Figure 2: Peptide maps of tryptic in-gel-digested A and B subunits of Stx2 and structural assignment.

SDS-PAGE and MALDI-TOF-MS of Stx2 as well as the data base search were performed exactly as described in Figure 1. All experimentally derived *m/z*-values of peaks 1 to 33 of Stx2A and peaks 1 to 9 of Stx2B were submitted to the data bases. The peptide mass search resulted in the identification of Stx2A (Shiga-like toxin II subunit A precursor, EC 3.2.2.22, rRNA *N*-glycosidase) encoded by the bacteriophage 933W composed of 319 amino acids with a molecular mass of 35,714 Da (accession number: P09385; excluding the signaling peptide: 297 amino acids, 33,195 Da) and Stx2B (Shiga-like toxin II subunit B) composed of 89 amino acids with a molecular mass of 9,874 Da (accession number: P09386, excluding the signaling peptide: 70 amino acids, 7,818 Da), both from *E. coli*. Those data fit well to the apparent molecular masses of ~32 kDa and ~7.7 kDa determined by SDS-PAGE for the A and B subunit, respectively. The database comparison of the submitted list of tryptic peptides resulted in a sequence coverage of 80.8% for Stx2A (highlighted in red) and 92.9% for Stx2B (highlighted in blue).



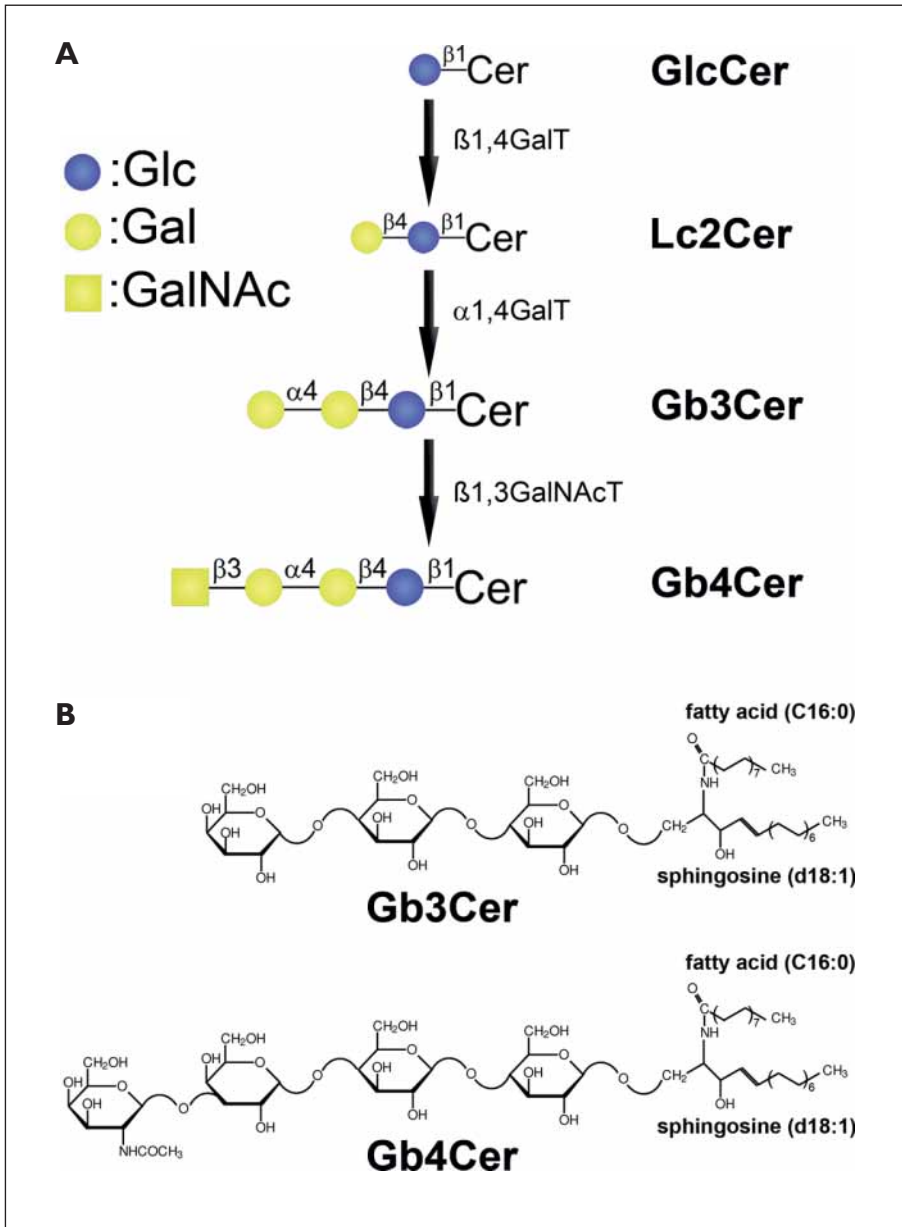


Figure 3: Biosynthesis flow diagram of globo-series neutral GSLs and structures of Gb3Cer and Gb4Cer. A) Glucosylceramide (GlcCer) is elongated by galactose through the action of β 1,4-galactosyltransferase (β 1,4GalT) yielding lactosylceramide (Lc2Cer). The α 1,4-galactosyltransferase (α 1,4GalT) or Gb3Cer synthase adds a galactose to Lc2Cer. Gb3Cer, the predominant receptor of Stx1 and Stx2, is then further elongated by β 1,3-*N*-acetylgalactosaminyltransferase (β 1,3GalNAcT) or Gb4Cer synthase which transfers *N*-acetylgalactosamine (GalNAc) to Gb3Cer. B) Structures of Gb3Cer and Gb4Cer depicted in the Haworth projection. Gb3Cer represents the high-affinity and Gb4Cer the low-affinity binding receptor for Stx1 and Stx2. Both neutral GSLs appear in human endothelial cells preferentially with C24 or C16 fatty acids but constant sphingosine (d18:1) in their ceramide parts, leading to typical double bands in thin-layer chromatograms (see Fig. 4).

GSLs are located primarily in microdomains of the plasma membrane of animal cells (76–78) also named lipid rafts (79). Their oligosaccharide chains spread in the aqueous environment at the cell surface and this makes them excellent candidates for cell surface recognition molecules (80, 81). Consequently, GSLs are involved in the pathophysiology of many infections and serve as receptors for viruses (82, 83), bacteria (84–86) and bacterial toxins including Stxs (87–90).

Stx1 and Stx2 both preferentially bind to the GSL Gb3Cer (91, 92) which alone is a functional receptor for Stx1 when incorporated in cells that lack Gb3Cer (93). Prototypic Stx1 and Stx2 bind with high affinity to Gb3Cer, where the Gal α 1–4Gal-terminus provides the specific recognition sequence for toxins' B pentamers. Both Stxs interact weakly with the tetrahexosylceramide globotetraosylceramide (Gb4Cer). Stx1 and Stx2 bind to Gb3Cer with similar specificity, but the oligosaccharide bind-

ing affinity of Stx1 is increased 10-fold compared to Stx2 (94). In addition, Stx1 and Stx2 exhibit differential association and dissociation rate constants: Stx2 binds to Gb3Cer more slowly than Stx1. However, once bound, Stx2 is difficult to dissociate as shown *in vitro* by surface plasmon resonance-based real-time receptor-binding analysis (95) (for biosynthesis and structures of globo-series neutral GSLs see Fig. 3). Differential binding properties may affect toxicities of Stx1 and Stx2 *in vivo* (96). However, not only the oligosaccharide part is important for toxin binding, but also the ceramide lipid anchor of the receptor (97, 98). The chain length and the degree of unsaturation and hydroxylation of the sphingosine base can vary, but the primary source of heterogeneity of the ceramide lies in the fatty acid composition. It has been shown that the length of the fatty acyl chain of Gb3Cer influences receptor function (99), intracellular sorting and retro-translocation of Stx to the cytosol (100, 101)

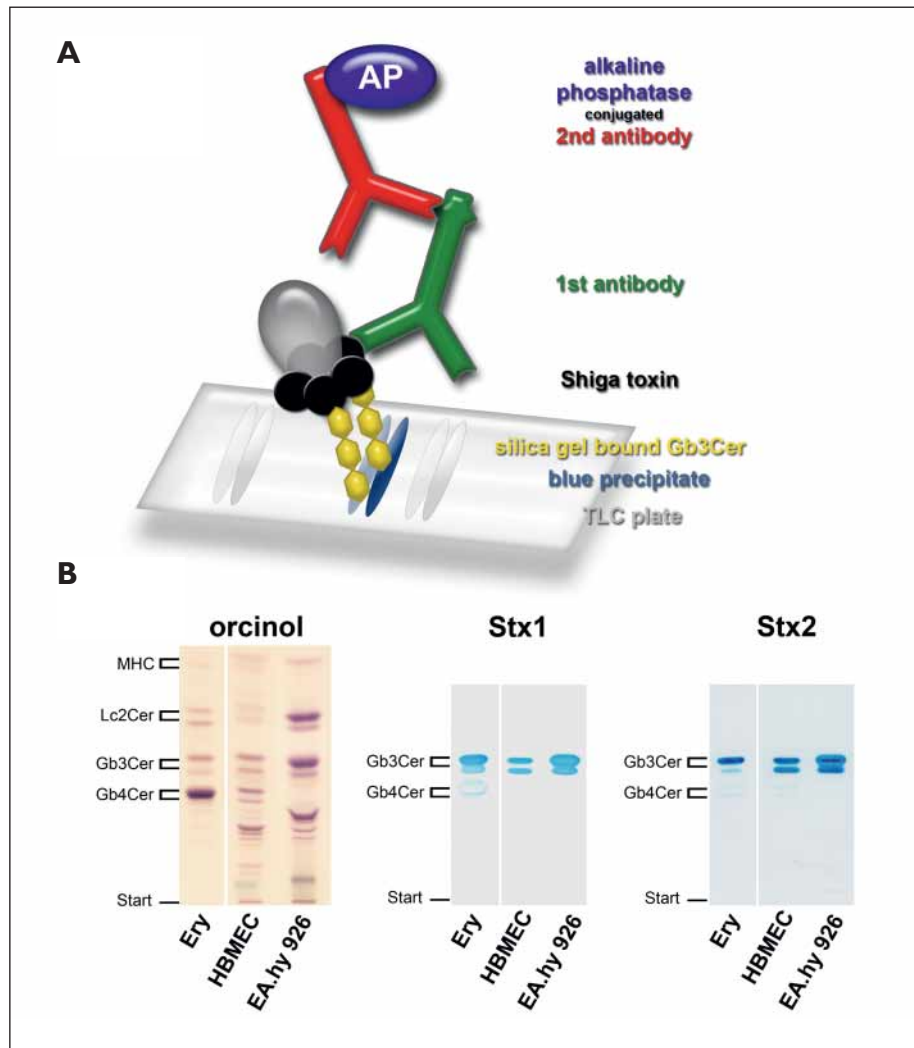


Figure 4: Scheme of the Stx TLC overlay assay and its application for detection of Stx1 and Stx2 receptors in human endothelial cells (139). A) GSLs are separated by TLC on silica gel precoated glass plates. After plastic fixation of the silica gel, the immobilized GSLs are overlaid with Stx solution, followed by incubation with primary anti-Stx antibody. Secondary enzyme-linked antibody (e.g. alkaline phosphatase) is required to visualize Stx-positive reaction by generating a coloured precipitate from a suitable substrate (e.g. 5-bromo-4-chloro-3-indolylphosphate). B) GSL extracts of HBMECs and EA.hy 926 cells were separated together with 20 μ g of neutral GSL references from human erythrocytes (Ery) as a positive control and stained with orcinol or subjected to Stx1 or Stx2 overlay assay. Applied GSLs correspond to 2×10^6 cells in the orcinol stain and to 5×10^5 cells in the Stx1 and Stx2 overlay assays. Vertical white lines indicate assembled non-contiguous lanes.

and nuclear targeting (46). Those data provide a molecular basis for the different pathology *in vivo* and suggest a previously unrecognized mechanism for the modulation of membrane GSL receptor function (7).

Stx1, Stx2, and their variants so far investigated bind preferentially to Gb3Cer with the exception of Stx2e. The latter toxin displays greater affinity to Gb4Cer compared to Gb3Cer (102–104). This difference in receptor binding is consistent with the difference in susceptibility of cell lines to the cytotoxicity of Stx2e and Gb3Cer-specific Stx1 and Stx2 (102). Thus, those toxins that are associated with human disease bind to Gb3Cer while Stx2e, which is associated with edema disease of swine, binds preferentially to Gb4Cer. In an elegant study performed by Lingwood et al., Gb3Cer binding specificity of Stx1 and Stx2 was converted to Gb4Cer and *vice versa* that for Stx2e from Gb4Cer to Gb3Cer by site-directed mutagenesis of the B subunits (105). The altered carbohydrate recognition of modified Stx2e from Gb4Cer to Gb3Cer has biological significance, resulting in Stx1-like disease after intravascular injection into pigs as compared with classical Stx2e-induced edema disease (106). These studies suggest the primary role of the carbohydrate bind-

ing specificity of Stxs in determining systemic pathology of STEC.

Stx receptors of endothelial cells

Binding of Stx to its receptor Gb3Cer on endothelial cells is postulated to be the critical event triggering the vascular injury caused by STEC (1, 4). At the target organs, Stxs bind through their B subunits to Gb3Cer, which is expressed in microvascular endothelial cells of the kidney (107), intestine (108), and brain (109). Variability in receptor expression has been ascribed to a number of factors including the degree of confluence of the cell culture (110, 111), cell-cycle-dependent regulation of GSL receptors (112, 113) and their tissue of origin, which is thought to reflect the different sensitivities observed *in vivo* (114). Though the importance of GSLs as receptors for Stxs is well documented, the exact GSL composition of endothelial cells has generally received low attention, and only limited data are available about the GSL composition of the various types of human endothelial cells. Most studies lack a detailed structural characterization of the relevant receptor GSLs and are limited to the immunological

detection of globo-series Gb3Cer and Gb4Cer using antibodies or Stxs, in combination with anti-Stx antibodies. The majority of investigations focused on human umbilical vein endothelial cells (HUVECs) (115, 116), where the neutral GSLs Gb3Cer and Gb4Cer were found to represent the dominant GSLs (117). We performed a thorough characterization of HUVEC GSLs using specific antibodies combined with methylation analysis and mass spectrometry (118). Gb4Cer and Gb3Cer, both carrying mainly C24 or C16 fatty acid beside sphingosine, were detected as the major neutral GSLs in HUVECs. The comparison of neutral GSLs from HUVECs and bovine aorta endothelial cells revealed striking differences in their GSL profiles. The predominance of neolacto-series and the absence of globo-series neutral GSLs are hallmarks of bovine aorta endothelial cells (119), which explains their resistance towards Stxs (120). As in HUVECs (110, 121), globo-series neutral GSLs were the major GSLs in primary and immortalized human brain microvascular endothelial cells (HBMECs) (122, 123). Upon stimulation with inflammatory mediators, an enhanced expression of Gb3Cer has been reported for HUVECs (114, 124, 125) and primary HBMECs from various sources (126–129) that correlated with increased Stx sensitivity. Thus, as with other cells, endothelial cell susceptibility to Stxs depends largely on Gb3Cer receptor expression. Differing Stx1 susceptibilities have been reported for endothelial cells from different vascular beds and species. The association between the degree of Stx sensitivity and Gb3Cer content is generally recognized (130).

Identification of Stx-receptors by overlay assay detection

Because of its resolving power and easy handling, high-performance thin-layer chromatography (TLC) has become the standard tool for separation and partial characterization of GSLs in mixtures (131–133). It is routinely used for analytical and preparative applications (134, 135). The oligosaccharide portions of GSLs can be visualized by conventional staining with orcinol after GSL-separation on silica gel precoated TLC plates. In conjunction with carbohydrate-binding proteins, such as antibodies or bacterial toxins, GSL species can be further differentiated in complex GSL mixtures by chromatographic resolution and subsequent immunodetection on the TLC plate (overlay assay) (136). The general procedure includes silica gel fixation with plastic to prevent flaking of the silica layer during incubation and washing steps, overlay of the plate with the primary agent (e.g. antibody or toxin), followed by incubation with secondary detection agents (e.g. alkaline phosphatase labeled antibody) and color development with a suitable substrate (e.g. 5-bromo-4-chloro-3-indolylphosphate). The schematic representation of the TLC overlay assay employing Stx is shown in Figure 4A. Figure 4B demonstrates its application to detect the receptors for Stx1 and Stx2 in two types of endothelial cells, human brain microvascular endothelial cells (HBMECs) and EA.hy 926 cells. EA.hy 926 cells represent “immortalized” macrovascular endothelial cells, which have been obtained by fusion of HUVECs with a human epithelial cell line (137). Both HBMECs (138) and EA.hy 926 cells have been widely used for endothelial cell re-

search ([139] and references therein). The orcinol stain of TLC separated GSL mixtures provides rather vague information about their individual GSLs, whereas specific cellular ligands of Stx1 and Stx2 can be easily identified in the GSL extracts of both cell lines by using the Stx overlay assay (Fig. 4B). Results from these experiments indicate that the two cell lines express different amounts of Gb3Cer, and that the major Gb3Cer species are distinguishable due to their chromatographic appearance as double bands. At this stage of investigation the upper and lower bands are supposed to represent Gb3Cer species with long- and short-chain fatty acids, respectively, whereas the sphingosine (d18:1) moiety of the ceramide is most likely constant and does not contribute to the structural heterogeneity of the lipid anchor (132, 133). We can further conclude from the TLC overlay assays of Figure 4B that both Stx1 and Stx2 exhibit identical binding specificity and preferentially bind to Gb3Cer, whereas Gb4Cer is only weakly stained in the reference mixture of neutral GSLs from human erythrocytes.

Structural characterization of Stx-receptors by mass spectrometry

MALDI-TOF-MS represents an excellent technology for sensitive mapping of GSL mixtures and structural characterization of their individual constituents (140, 141). GSL differences observed by TLC overlay assay with antibody or toxin binding (see Fig. 4) can be verified and structurally characterized by conventional ultraviolet (UV)-MALDI-TOF-MS. For this purpose the plastic fixative is removed from the silica gel layer by chloroform extraction, and immunopositive GSL bands of interest are scraped from the support and extracted as described in detail in previous publications (142, 143). This combined preparative TLC-MS technology requires only microgram quantities of GSL mixtures. Our group applied this strategy successfully to the structural characterization of Gb3Cer and Gb4Cer species from human erythrocytes with high- and low-affinity binding to Stx1, respectively (143). For many applications, these newer, joint TLC-MS strategies can replace the laborious and time-consuming HPLC purification of single GSLs (144). Following the outlined strategy, we analyzed Stx-stained GSLs from HBMECs and EA.hy 926 cells by MALDI-TOF-MS. Crude GSL extracts from both cell lines (Fig. 4) are sufficient to generate MALDI-TOF mass spectra as shown in Figure 5. The main species detected in both spectra correspond to the monosodiated $[M+Na]^+$ molecular ions of Gb3Cer (d18:1, C16:0) and Gb3Cer (d18:1, C24:1/C24:0) accompanied by low abundance ions indicative of Gb3Cer (d18:1, C22:0). In contrast to HBMECs, minor Gb3Cer-species containing C26:1- and C26:0-fatty acids were noted in EA.hy 926 cells. The data demonstrate that HBMECs contain almost equal amounts of Gb3Cer species with long- and short-chain fatty acids. In contrast, Gb3Cer spectra of EA.hy 926 cells demonstrated a relative increase of long-chain fatty acids. Gb3Cer species with saturated C24:0 fatty acid predominated over those with unsaturated C24:1 fatty acids in EA.hy 926 cells, while HBMECs showed a balanced ratio of these fatty acids. It has been suggested that Gb3Cer species with long-chain fatty acids display greater sensitivity to Stx-mediated cytotoxicity,

likely because they may more effectively mediate the localization of internalized toxin to the ER (145). Differences in the overall GSL composition of Stx-sensitive and resistant cells that express Gb3Cer species of apparently identical composition may also affect Gb3Cer recognition by and sorting of incorporated Stx1 (146).

It should be noted that GSLs can be directly analysed from silica gel plates by TLC-IR (infrared)-MALDI-TOF-MS of fluorochrome- or antibody-stained GSLs (147, 148). Thus, the TLC-overlay assay combined with mass spectrometry represents the state of the art to structurally characterize Stx-receptors from any biological sources, including primary cells, cell lines, or organ tissue. Figure 6 shows an example for the identification of Stx-receptors in human kidney and colon based on Stx1 TLC overlay assays and the corresponding MALDI mass spectra obtained from extracts of both tissues. As expected (149), human kidney shows a high concentration of Stx1-binding Gb3Cer receptors, while there is only scant expression of Gb3Cer in human colon (Fig. 6A). This difference is reflected by the corresponding MS signal intensities of Gb3Cer ions in kidney and colon (Fig.

6B and C, respectively). The different Gb3Cer species varying in their fatty acid substitution from C16 up to C24 acyl chain length are speculated to derive mostly from endothelial and epithelial cells of those organs.

The role of lipid rafts and caveolae in Stx binding, internalization, and retrograde transport

Many investigators have provided evidence for the existence of cholesterol-sphingolipid-enriched microenvironments on the cell surface – known as lipid rafts – which renders the membrane more ordered and less fluid than the bulk plasma membrane. Rafts are rich in GSLs, cholesterol, lipid-modified proteins (e.g. GPI-anchored proteins, doubly acylated Src-type kinases) and transmembrane proteins (150). The raft concept has long been controversial, but studies with improved methodologies have dispelled most doubts (79, 151, 152). Furthermore, evidence has accumulated that GSLs, specifically enriched in the exoplasmic

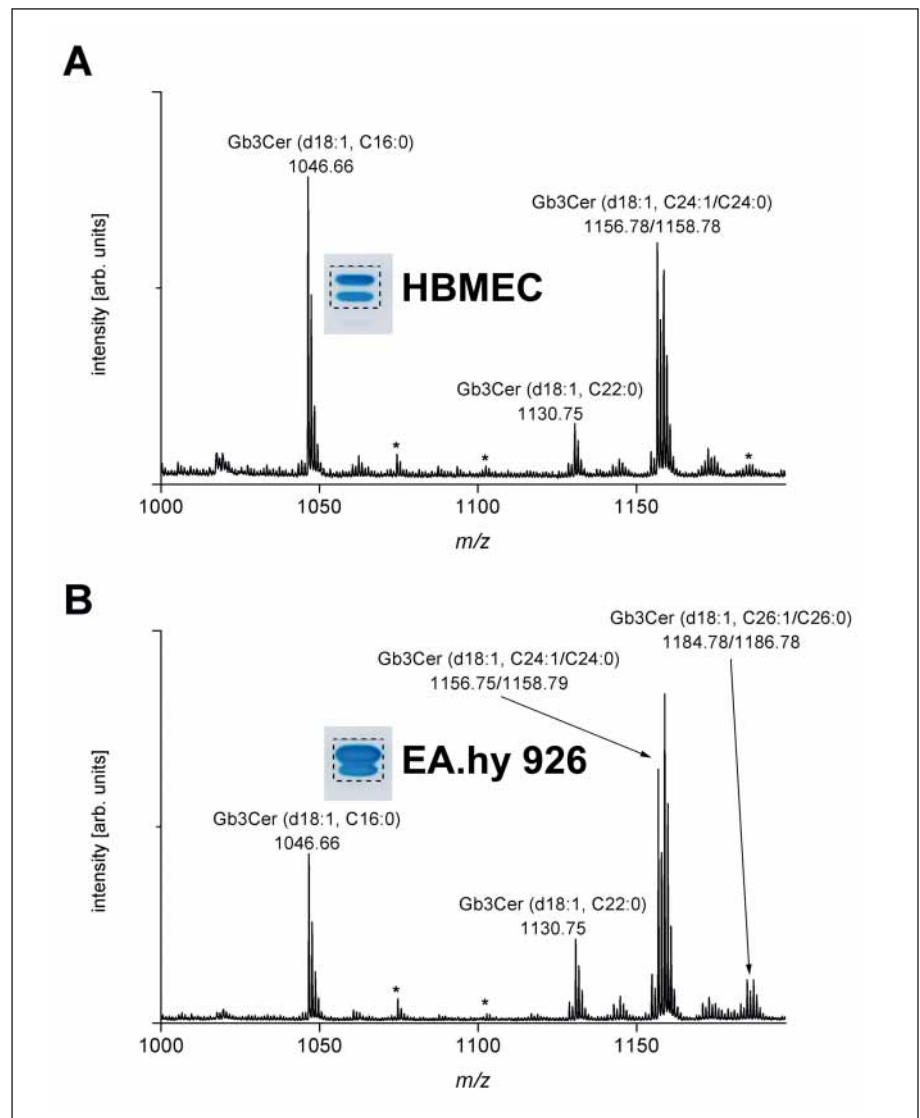


Figure 5: Structural characterization of Stx1-detected Gb3Cer species in HBMECs (A) and EA.hy 926 cells (B) by MALDI-TOF-MS. The Stx1 TLC overlay assays were performed as described in Figure 4 and the Stx1 positive bands, from which the GSLs were extracted for subsequent MALDI-TOF-MS, are shown in the dotted rectangles of the insets. Mass spectra from extracts equivalent to 7×10^4 cells were acquired in the positive ion mode and all Gb3Cer species were detected as singly charged mono-sodiated ions. The minor signals marked with asterisks represent Gb3Cer species carrying C18 to C26 fatty acids assigned by shifts in 28 atomic mass units in comparison to major molecular ions.

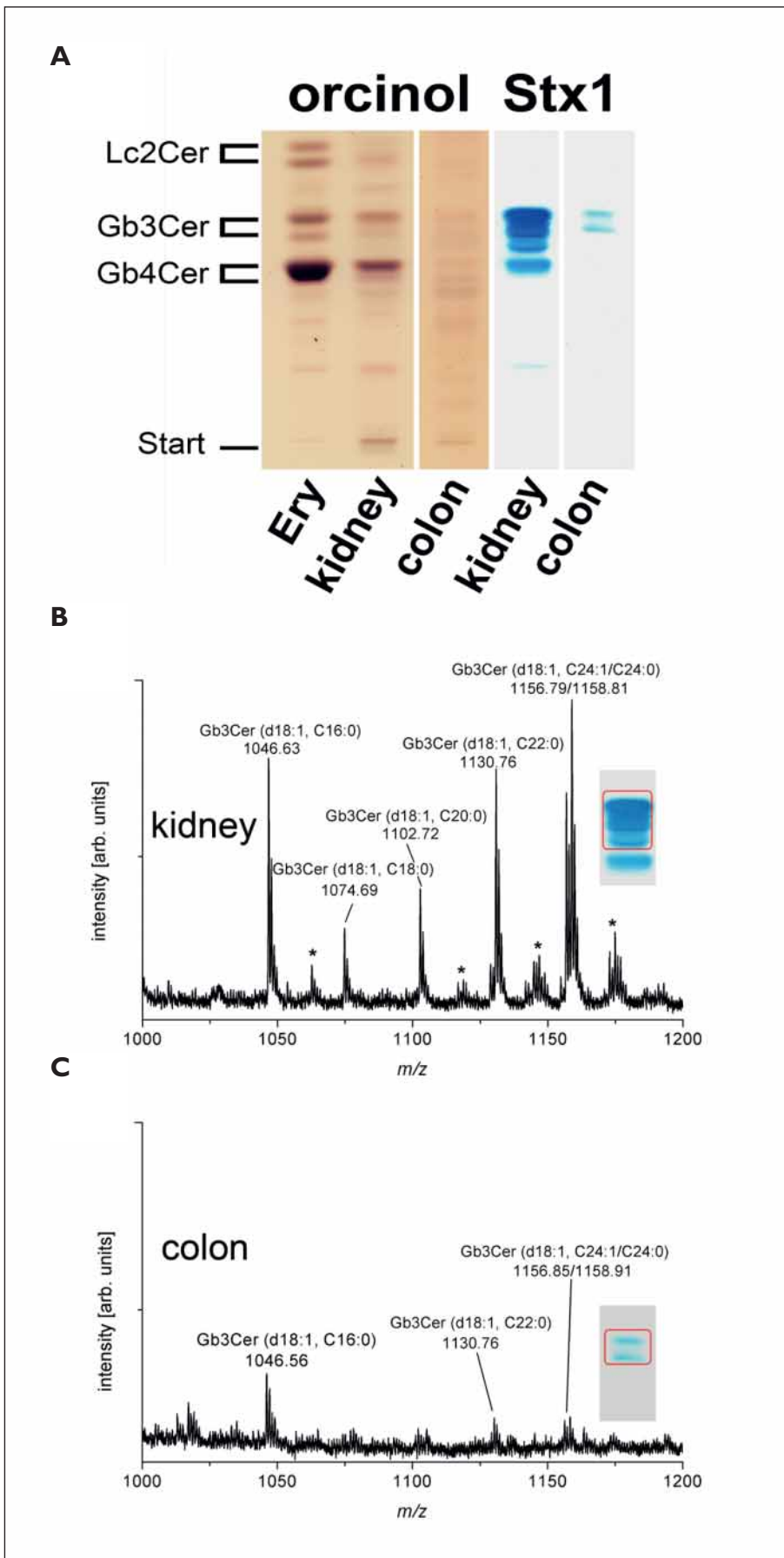


Figure 6: Structural characterization of StxI-detected receptors in human kidney and colon. A) The orcinol stains and StxI overlay assays of TLC separated GSL extracts from representative kidney and colon tissue samples were performed as described in Figure 4. Applied GSLs correspond to 2 mg of wet weight tissue. B, C) MALDI-TOF-MS was performed with extracts from StxI positive bands (see dotted rectangles in the inserts) that correspond to 30 μ g of kidney (B) and 3 mg of colon wet weight tissue (C). Mass spectra were acquired in the positive ion mode and all Gb3Cer species were detected as singly charged mono-sodiated ions. The signals marked with asterisks in the kidney spectrum, which show a remarkable shift in 16 atomic mass units in comparison to major molecular ions, are assumed to represent related hydroxylated Gb3Cer species. The positions of postulated hydroxylation in the ceramide portions are yet unknown, and the exact localization requires further investigation of each single GSL by tandem mass spectrometry. The StxI overlay assay of the kidney extract suggests functioning of the hydroxylated Gb3Cer species as StxI receptors. The question whether this modification is specific for the kidney cannot be answered without further structural characterization of a representative number of kidney samples.

leaflet of the plasma membrane, exert an important function as platform for the initiation of signaling cascades (153, 154).

Caveolae comprise one subset of lipid rafts in cell surface (150, 152, 155, 156). These flask-shaped membrane invaginations are formed from lipid rafts by polymerization of caveolins, which are hairpin-like palmitoylated integral membrane proteins that tightly bind cholesterol and sphingolipids (157). Endothelial cells are among the richest in caveolae. Caveolae have been found to be partake in many physiological and pathological processes involving endothelial cells, such as atherosclerosis, hemostasis, and thrombosis (158, 159). Caveolae and rafts are internalized via a common pathway, caveolae/raft-dependent endocytosis. This pathway is clathrin-independent and sensitive to cholesterol depletion (160, 161). Studies that investigated the role of lipid rafts in Stx1-interaction with various cell types demonstrated the clustering of Gb3Cer in lipid rafts (162) and, moreover, binding of Stx B-subunit with raft-localized receptors as a requirement for the retrograde transport (163). Binding of Stx to Gb3Cer induces activation of the Src family kinase Yes and intracellular signals that mediate cytoskeleton remodeling (164, 165). Furthermore, the association of Stx1-Gb3Cer-interaction with a precursor of Gb3Cer, glucosylceramide, is an essential requirement for a cytotoxic effect in the ER (166). Moreover, different pools of Gb3Cer have been described that are thought to influence not only Stx cell binding, but also to affect intracellular trafficking of the toxin (167). These data suggest that only GSLs that associate strongly with lipid rafts carry AB₅ toxins retrogradely from the plasma membrane and sort the toxins to the ER (168).

Despite vast data concerning protein assembly in lipid rafts and caveolae of various cell types, little is known about their GSL composition. As outlined above, the oligosaccharide portion of Gb3Cer determines its binding specificity towards Stxs, but the ceramide contributes to Stx binding properties through its fatty acid heterogeneity. Available evidence also suggests that the structure of the ceramide moiety defines the preferential occurrence of GSLs in the liquid-ordered or liquid-disordered phase of the plasma membrane and the strength of the association of GSLs and toxins with lipid rafts (151). Such biophysical features of the lipid moiety of GSL receptors may influence its incorporation into certain membrane domains, the retrograde intracellular route and thus may affect toxin destination.

References

- Karch H, et al. Enterohaemorrhagic *Escherichia coli* in human medicine. *Int J Med Microbiol* 2005; 295: 405–418.
- Karmali MA. Infection by Shiga toxin-producing *Escherichia coli*: an overview. *Mol Biotechnol* 2004; 26: 117–122.
- Tarr PI, et al. Shiga toxin-producing *Escherichia coli* and the haemolytic uraemic syndrome. *Lancet* 2005; 365: 1073–1086.
- Bielaszewska M, Karch H. Consequences of enterohaemorrhagic *Escherichia coli* infection for the vascular endothelium. *Thromb Haemost* 2005; 94: 312–318.
- Barbieri L, et al. Shiga-like toxin I is a polynucleotide:adenosine glycosidase. *Mol Microbiol* 1998; 29: 661–662.
- Brigotti M, et al. Damage to nuclear DNA induced by Shiga toxin 1 and ricin in human endothelial cells. *FASEB J* 2002; 16: 365–372.
- Sandvig K. Shiga toxins. *Toxicon* 2001; 39: 1629–1635.
- Jackson MP, et al. Nucleotide sequence analysis and comparison of the structural genes for Shiga-like toxin I and Shiga-like toxin II encoded by bacteriophages from *Escherichia coli* 933. *FEMS Microbiol Lett* 1987; 44: 109–114.
- Friedrich AW, et al. *Escherichia coli* harboring Shiga toxin 2 gene variants: frequency and association with clinical symptoms. *J Infect Dis* 2002; 185: 74–84.
- Friedrich AW, et al. Shiga toxin 1c-producing *Escherichia coli* strains: Phenotypic and genetic characterization and association with human disease. *J Clin Microbiol* 2003; 41: 2448–2453.
- Bielaszewska M, et al. Shiga toxin activatable by intestinal mucus in *Escherichia coli* isolated from humans: predictor for a severe clinical outcome. *Clin Infect Dis* 2006; 43: 1160–1167.
- Zhang W, et al. Structural and functional differences between disease-associated genes of enterohaemorrhagic *Escherichia coli* O111. *Int J Med Microbiol* 2007; 297: 17–26.
- Orth D, et al. The Shiga toxin genotype rather than the amount of Shiga toxin or the cytotoxicity of Shiga toxin in vitro correlates with the appearance of the hemolytic uraemic syndrome. *Diagn Microbiol Infect Dis* 2007; 59: 235–242.
- Jenkins C, et al. Subtyping of virulence genes in verocytotoxin-producing *Escherichia coli* (VTEC) other than serogroup O157 associated with disease in the United Kingdom. *J Med Microbiol* 2003; 52: 941–947.

Table 1: Shiga toxins produced by human STEC isolates and their disease association.

Stx gene	Stx protein	Disease association ^a	Reference
stx ₁	Stx1	D, BD, HUS, A	9, 13, 172
stx _{1c}	Stx1c	D, BD, HUS, A	10, 13, 18
stx _{1d}	Stx1d	D	20
stx ₂	Stx2	D, BD, HUS	9, 13, 14, 17, 33, 172–174
stx _{2c}	Stx2c	D, BD, HUS	9, 13, 14, 172
stx _{2c2}	Stx2c2	D	22
stx _{2d}	Stx2d	D, A	9, 13, 14, 23
stx _{2d-activatable}	Stx2d _{activatable}	D, BD, HUS	11, 13, 16, 29
stx _{2e}	Stx2e	D, A	9, 13, 25
stx _{2f}	Stx2f	D	14, 26–28, 32

^a D, watery diarrhea without visible blood; BD, diarrhea with visible blood; HUS, haemolytic uraemic syndrome; A, asymptomatic shedding.

Perspectives

HUS is a thrombotic disorder. Insights into toxin-receptor interactions and, specifically, the mechanism(s) of Stx-mediated cell injury that induces a prothrombotic response, are important goals. Endothelial cells, particularly those with high globoseries GSL content are plausibly the major target in STEC-related disease. Future investigations aimed at advancing our understanding of the subcellular lipid raft distribution in endothelial cell membranes, will be aided by novel biochemical and biophysical strategies (169, 170). This research will allow us to better understand the complex mechanisms of Stx binding and internalization, and may help to develop new strategies directed at the interruption of the Stx-induced pathological intracellular cascades.

Acknowledgements

We thank Martin Bitzan (Montreal Children's Hospital/McGill University, Montreal, QC, Canada) for critical reading of the manuscript and stimulating discussions.

15. Boerlin P, et al. Association between virulence factors of Shiga toxin-producing *Escherichia coli* and disease in human. *J Clin Microbiol* 1999; 37: 497–503.
16. Beutin L, et al. Characterization of Shiga toxin-producing *Escherichia coli* strains isolated from humans in Germany over a 3-year period. *J Clin Microbiol* 2004; 42: 1099–1108.
17. Brooks JT, et al. Non-O157 Shiga toxin-producing *Escherichia coli* infections in the United States, 1983–2002. *J Infect Dis* 2005; 192: 1422–1429.
18. Zhang W, et al. Identification, characterization and distribution of a Shiga toxin 1 gene variant (*stx_{1c}*) in *Escherichia coli* isolated from humans. *J Clin Microbiol* 2002; 40: 1441–1446.
19. Bürk C, et al. Identification and characterization of a new variant of Shiga toxin 1 in *Escherichia coli* O157:H7 of bovine origin. *J Clin Microbiol* 2003; 41: 2106–2112.
20. Kuczias T, et al. A rapid method for the discrimination of genes encoding classical Shiga toxin (Stx) 1 and its variants, Stx1c and Stx1d, in *Escherichia coli*. *Mol Nutr Food Res* 2004; 48: 515–521.
21. Schmitt CK, et al. Two copies of Shiga-like toxin II-related genes common in enterohemorrhagic *Escherichia coli* strains are responsible for the antigenic heterogeneity of the O157:H⁺ strain E32511. *Infect Immun* 1991; 59: 1065–1073.
22. Jelacic JK, et al. Shiga toxin-producing *Escherichia coli* in Montana: bacterial genotypes and clinical profiles. *J Infect Dis* 2003; 188: 719–729.
23. Pierard D, et al. Identification of new verocytotoxin type 2 variant B-subunit genes in human and animal *Escherichia coli* isolates. *J Clin Microbiol* 1998; 36: 3317–3322.
24. Melton-Celsa AR, et al. Activation of Shiga-like toxins by mouse and human intestinal mucus correlates with virulence of enterohemorrhagic *Escherichia coli* O91:H21 isolates in orally infected, streptomycin-treated mice. *Infect Immun* 1996; 64: 1569–1576.
25. Sonntag AK, et al. Shiga toxin 2e-producing *Escherichia coli* isolates from humans and pigs differ in their virulence profiles and interactions with intestinal epithelial cells. *Appl Environ Microbiol* 2005; 71: 8855–8863.
26. Sonntag AK, et al. Pigeons as a possible reservoir of Shiga toxin 2f-producing *Escherichia coli* pathogenic to humans. *Berl Munch Tierarztl Wochenschr* 2005; 118: 464–470.
27. Seto K, et al. Biochemical and molecular characterization of minor serogroups of Shiga toxin-producing *Escherichia coli* isolated from humans in Osaka prefecture. *J Vet Med Sci* 2007; 69: 1215–1222.
28. van Duynhoven YT, et al. Prevalence, characterization and clinical profiles of Shiga toxin-producing *Escherichia coli* in The Netherlands. *Clin Microbiol Infect* 2008; 14: 437–445.
29. Prager R, et al. Diversity of virulence patterns among Shiga toxin-producing *Escherichia coli* from human clinical cases – need for more detailed diagnostics. *Int J Med Microbiol* 2005; 295: 29–38.
30. Mellmann A, et al. Analysis of the collection of hemolytic uremic syndrome-associated enterohemorrhagic *Escherichia coli* (HUSEC). *Emerg Infect Dis* 2008; 14: 1287–1290.
31. Schmidt H, et al. A new Shiga toxin 2 variant (Stx2f) from *Escherichia coli* isolated from pigeons. *Appl Environ Microbiol* 2000; 66: 1205–1208.
32. Isobe J, et al. Isolation of *Escherichia coli* O128:HNM harboring *stx2f* gene from diarrhea patients. *Kansenshogaku Zasshi* 2004; 78: 1000–1005.
33. Mellmann A, et al. Recycling of Shiga toxin 2 genes in sorbitol-fermenting enterohemorrhagic *Escherichia coli* O157:NM. *Appl Environ Microbiol* 2008; 74: 67–72.
34. Bielaszewska M, et al. Shiga toxin gene loss and transfer in vitro and in vivo during enterohemorrhagic *Escherichia coli* O26 infection in humans. *Appl Environ Microbiol* 2007; 73: 3144–3150.
35. Bielaszewska M, et al. Shiga toxin-mediated hemolytic uremic syndrome: time to change the diagnostic paradigm? *PLoS ONE* 2007; 2:e1024.
36. Friedrich AW, et al. Prevalence, virulence profiles, and clinical significance of Shiga toxin-negative variants of enterohemorrhagic *Escherichia coli* O157 infection in humans. *Clin Infect Dis* 2007; 45: 39–45.
37. Bielaszewska M, et al. Shiga toxin-negative attaching and effacing *Escherichia coli*: distinct clinical associations with bacterial phylogeny and virulence traits and inferred in-host pathogen evolution. *Clin Infect Dis* 2008; 47: 208–217.
38. Endo Y, et al. Site of action of a Vero toxin (VT2) from *Escherichia coli* O157:H7 and Shiga toxin on eukaryotic ribosomes. *Eur J Biochem* 1988; 171: 45–50.
39. Ling H, et al. Structure of the Shiga-like toxin I B-pentamer complexed with an analogue of its receptor Gb₃. *Biochemistry* 1998; 37: 1777–1788.
40. Paton JC, Paton AW. Shiga toxin ‘goes retro’ in human primary kidney cells. *Kidney Int* 2006; 70: 2049–2051.
41. Sandvig K, et al. Pathways followed by ricin and Shiga toxin into cells. *Histochem Cell Biol* 2002; 117: 131–141.
42. Bonifacino JS, Rojas R. Retrograde transport from endosomes to the trans-Golgi network. *Nat Rev Mol Cell Biol* 2006; 7: 568–579.
43. Römer W, et al. Shiga toxin induces tubular membrane invaginations for its uptake into cells. *Nature* 2007; 450: 670–675.
44. Sandvig K, et al. Retrograde transport of endocytosed Shiga toxin to the endoplasmic reticulum. *Nature* 1992; 358: 510–512.
45. Lingwood CA. Role of verotoxin receptors in pathogenesis. *Trends Microbiol* 1996; 4: 147–153.
46. Arab S, Lingwood CA. Intracellular targeting of the endoplasmic reticulum/nuclear envelope by retrograde transport may determine cell hypersensitivity to verotoxin via globotriaosyl ceramide fatty isoform traffic. *J Cell Physiol* 1998; 177: 646–660.
47. Garred Ø, et al. Furin-induced cleavage and activation of Shiga toxin. *J Biol Chem* 1995; 270: 10817–10821.
48. Lea N, et al. Proteolytic cleavage of the A subunit is essential for maximal cytotoxicity of *Escherichia coli* O157:H7 Shiga-like toxin-1. *Microbiology* 1999; 145: 999–1004.
49. Tam PJ, Lingwood CA. Membrane-cytosolic translocation of verotoxin A₁ subunit in target cells. *Microbiology* 2007; 153: 2700–2710.
50. Obrug TG. Shiga toxin mode of action in *E. coli* O157:H7 disease. *Front Biosci* 1997; 2: d635–642.
51. Cherla RP, et al. Shiga toxins and apoptosis. *FEMS Microbiol Lett* 2003; 228: 159–166.
52. Nakao H, Takeda T. *Escherichia coli* Shiga toxin. *J Nat Toxins* 2000; 9: 299–313.
53. Karch H. The role of virulence factors in enterohemorrhagic *Escherichia coli* (EHEC)-associated hemolytic-uremic syndrome. *Semin Thromb Hemost* 2001; 27: 207–213.
54. Forsyth KD, et al. Neutrophil-mediated endothelial injury in haemolytic uraemic syndrome. *Lancet* 1989; 2: 411–414.
55. Morigi M, et al. Verotoxin-1-induced up-regulation of adhesive molecules renders microvascular endothelial cells thrombogenic at high shear stress. *Blood* 2001; 98: 1828–1835.
56. Morigi M, et al. Verotoxin-1 promotes leucocyte adhesion to cultured endothelial cells under physiologic flow conditions. *Blood* 1995; 86: 4553–4558.
57. Mulvey G, et al. Affinity purification of Shiga-like toxin I and Shiga-like toxin II. *J Microbiol Methods* 1998; 32: 247–252.
58. Nakajima H, et al. Single-step method for purification of Shiga toxin-1 B subunit using receptor-mediated affinity chromatography by globotriaosylceramide-conjugated octyl sepharose CL-4B. *Protein Expr Purif* 2001; 22: 267–275.
59. Boulanger J, et al. Universal method for the facile production of glycolipid/lipid matrices for the affinity purification of binding ligands. *Anal Biochem* 1994; 217: 1–6.
60. Karch H, Bitzan M. Purification and characterization of a phage-encoded cytotoxin from an *Escherichia coli* O111 strain associated with hemolytic-uremic syndrome. *Zentralbl Bakteriol Mikrobiol Hyg* 1988; 270: 41–51.
61. Karch H, et al. Purified verotoxins of *Escherichia coli* O157:H7 decrease prostacyclin synthesis by endothelial cells. *Microb Pathog* 1988; 5: 215–221.
62. Shevchenko A, et al. Mass spectrometric sequencing of proteins from silver-stained polyacrylamide gels. *Anal Chem* 1996; 68: 850–858.
63. Aebersold R, Goodlett DR. Mass spectrometry in proteomics. *Chem Rev* 2001; 101: 269–295.
64. Fraser ME, et al. Structure of Shiga toxin type 2 (Stx2) from *Escherichia coli* O157:H7. *J Biol Chem* 2004; 279: 27511–27517.
65. Shayman JA, Radin NS. Structure and function of renal glycosphingolipids. *Am J Physiol* 1991; 260: F291–302.
66. Holgersson J, Jovall PA. Glycosphingolipids of human large intestine: detailed structural characterization with special reference to blood group compounds and bacterial receptor structures. *J Biochem* 1991; 110: 120–131.
67. Macher BA, et al. Glycosphingolipids of normal and leukemic human leukocytes. *Mol Cell Biochem* 1982; 47: 81–95.
68. Gillard BK, et al. Association of glycosphingolipids with intermediate filaments of mesenchymal, epithelial, glial, and muscle cells. *Cell Motil Cytoskeleton* 1992; 21: 255–271.
69. Feizi T. Carbohydrate differentiation antigens: probable ligands for cell adhesion molecules. *Trends Biochem Sci* 1991; 16: 84–86.
70. Erdmann M, et al. Differential surface expression and possible function of 9-O- and 7-O-acetylated GD3 (CD60 b and c) during activation and apoptosis of human tonsillar B and T lymphocytes. *Glycoconj J* 2006; 23: 627–638.
71. Alessandri G, et al. Growth and motility of microvascular endothelium are modulated by the relative concentration of gangliosides in the medium. *J Cell Physiol* 1992; 151: 23–28.
72. Lahiri S, Futerman AH. The metabolism and function of sphingolipids and glycosphingolipids. *Cell Mol Life Sci* 2007; 64: 2270–2284.
73. Schnaar RL. Glycolipid-mediated cell-cell recognition in inflammation and nerve regeneration. *Arch Biochem Biophys* 2004; 426: 163–172.
74. Stults CL, et al. Glycosphingolipids: structure, biological source, and properties. *Methods Enzymol* 1989; 179: 167–214.
75. Müthing J. Mammalian glycosphingolipids. In: *Glycoscience: Chemistry and Chemical Biology*. Vol 3. Heidelberg, Germany: Springer-Verlag 2001; 2220–2249.
76. Fantini J, et al. Glycosphingolipid (GSL) microdomains as attachment platforms for host pathogens and their toxins on intestinal epithelial cells: activation of signal transduction pathways and perturbations of intestinal absorption and secretion. *Glycoconj J* 2000; 17: 173–179.

77. Hakomori SI. Cell adhesion/recognition and signal transduction through glycosphingolipid microdomain. *Glycoconj J* 2000; 17: 143–151.
78. Sonnino S, et al. Dynamic and structural properties of sphingolipids as driving forces for the formation of membrane domains. *Chem Rev* 2006; 106: 2111–2125.
79. Simons K, Toomre D. Lipid rafts and signal transduction. *Nat Rev Mol Cell Biol* 2000; 1: 31–41.
80. Schnaar RL. Glycosphingolipids in cell surface recognition. *Glycobiology* 1991; 1: 477–485.
81. Feizi T. Carbohydrate-mediated recognition systems in innate immunity. *Immunol Rev* 2000; 173: 79–88.
82. Russel RJ, et al. Avian and human receptor binding by hemagglutinins of influenza A viruses. *Glycoconj J* 2006; 23: 85–92.
83. Hidari KIPJ, et al. Binding kinetics of influenza viruses to sialic acid-containing carbohydrates. *Glycoconj J* 2007; 24: 583–590.
84. Karlsson KA. Animal glycosphingolipids as membrane attachment sites for bacteria. *Annu Rev Biochem* 1989; 58: 309–350.
85. Teneberg S, et al. Carbohydrate recognition by enterohemorrhagic *Escherichia coli*: characterization of a novel glycosphingolipid from cat small intestine. *Glycobiology* 2004; 14: 187–196.
86. Miller-Podraza H, et al. Novel binding epitope for *Helicobacter pylori* found in neolacto carbohydrate chains: structure and cross-binding properties. *J Biol Chem* 2005; 280: 19695–19703.
87. Usuki S, et al. Chemical validation of molecular mimicry: interaction of cholera toxin with *Campylobacter* lipooligosaccharides. *Glycoconj J* 2007; 24: 167–180.
88. Merrit EA, Hol WG. AB₅ toxins. *Curr Opin Struct Biol* 1995; 5: 165–171.
89. Yowler BC, Schengrund CL. Glycosphingolipids – sweets for botulinum neurotoxin. *Glycoconj J* 2004; 21: 287–293.
90. Smith DC, et al. Glycosphingolipids as toxin receptors. *Semin Cell Dev Biol* 2004; 15: 397–408.
91. Lingwood CA, et al. Glycolipid binding of purified and recombinant *Escherichia coli* produced verotoxin *in vitro*. *J Biol Chem* 1987; 262: 8834–8839.
92. Waddell T, et al. Globotriose ceramide is specifically recognized by the *Escherichia coli* Verocytotoxin 2. *Biochem Biophys Res Commun* 1988; 152: 674–679.
93. Waddell T, et al. Induction of verotoxin sensitivity in receptor-deficient cell lines using the receptor glycolipid globotriaosylceramide. *Proc Natl Acad Sci USA* 1990; 87: 7898–7901.
94. Head SC, et al. Preparation of VT1 and VT2 hybrid toxins from their purified dissociated subunits. Evidence for B subunit modulation of a subunit function. *J Biol Chem* 1991; 266: 3617–3621.
95. Nakajima H, et al. Kinetic analysis of binding between Shiga toxin and receptor glycolipid Gb3Cer by surface plasmon resonance. *J Biol Chem* 2001; 276: 42915–42922.
96. Louise CB, Obrig TG. Specific interaction of *Escherichia coli* O157:H7-derived Shiga-like toxin II with human renal endothelial cells. *J Infect Dis* 1995; 172: 1397–1401.
97. Boyd B, et al. Lipid modulation of glycolipid receptor function. *Eur J Biochem* 1994; 223: 873–878.
98. Binnington B, et al. Effect of globotriaosylceramide fatty acid α -hydroxylation on the binding by verotoxin 1 and verotoxin 2. *Neurochem Res* 2002; 27: 807–813.
99. Kiarash A, et al. Glycosphingolipid receptor function is modified by fatty acid content. *J Biol Chem* 1994; 269: 11138–11146.
100. Lingwood CA. Aglycone modulation of glycolipid receptor function. *Glycoconj J* 1996; 13: 495–503.
101. Sandvig K, et al. Importance of glycolipid synthesis for butyric acid-induced sensitization to Shiga toxin and intracellular sorting of toxin in A431 cells. *Mol Biol Cell* 1996; 7: 1391–1404.
102. DeGrandis S, et al. Globotetraosylceramide is recognized by the pig edema disease toxin. *J Biol Chem* 1989; 264: 12520–12525.
103. Samuel JE, et al. Comparison of the glycolipid receptor specificities of Shiga-like toxin type II and Shiga-like toxin type II variants. *Infect Immun* 1990; 58: 611–618.
104. Waddell TE, et al. Interaction of verotoxin 2e with pig intestine. *Infect Immun* 1996; 64: 1714–1719.
105. Tyrrell GJ, et al. Alteration of the carbohydrate binding specificity of verotoxins from Gal α 1–4Gal to GalNAc β 1–3Gal α 1–4Gal and vice versa by site-directed mutagenesis of the binding subunit. *Proc Natl Acad Sci USA* 1992; 89: 524–528.
106. Boyd B, et al. Alteration of the glycolipid binding specificity of the pig edema toxin from globotetraosyl to globotriaosyl ceramide alters *in vivo* tissue targeting and results in a verotoxin 1-like disease in pigs. *J Exp Med* 1993; 177: 1745–1753.
107. Boyd B, Lingwood C. Verotoxin receptor glycolipid in human renal tissue. *Nephron* 1989; 51: 207–210.
108. Jacewicz M, et al. Responses of human intestinal microvascular endothelial cells to Shiga toxins 1 and 2 and pathogenesis of hemorrhagic colitis. *Infect Immun* 1999; 67: 1439–1444.
109. Ren J, et al. Localization of verotoxin receptors in nervous system. *Brain Res* 1999; 825: 183–188.
110. Obrig TO, et al. Direct cytotoxic action of Shiga toxin on human vascular endothelial cells. *Infect Immun* 1988; 56: 2373–2378.
111. van Setten PA, et al. Effects of TNF α on verocytotoxin cytotoxicity in purified human glomerular microvascular endothelial cells. *Kidney Int* 1997; 51: 1245–1256.
112. Pudymaitis A, Lingwood CA. Susceptibility to verotoxin as a function of the cell cycle. *J Cell Physiol* 1992; 150: 632–639.
113. Majouli I, et al. Differential expression of receptors for Shiga and Cholera toxin is regulated by the cell cycle. *J Cell Sci* 2002; 115: 817–826.
114. Obrig TG, et al. Endothelial heterogeneity in Shiga toxin receptors and responses. *J Biol Chem* 1993; 268: 15484–15488.
115. Gillard BK, et al. Association of glycosphingolipids with intermediate filaments of human umbilical vein endothelial cells. *Exp Cell Res* 1991; 192: 433–444.
116. Gillard BK, et al. Variable subcellular localization of glycosphingolipids. *Glycobiology* 1993; 3: 57–67.
117. Gillard BK, et al. Glycosphingolipids of human umbilical vein endothelial cells and smooth muscle cells. *Arch Biochem Biophys* 1987; 256: 435–445.
118. Müthing J, et al. Isolation and structural characterization of glycosphingolipids of *in vitro* propagated human umbilical vein endothelial cells. *Glycobiology* 1999; 9: 459–468.
119. Duvar S, et al. Isolation and structural characterization of glycosphingolipids of *in vitro* propagated bovine aortic endothelial cells. *Glycobiology* 1997; 7: 1099–1109.
120. Ohmi K, et al. Human microvascular endothelial cells are strongly sensitive to Shiga toxins. *Biochem Biophys Res Commun* 1998; 251: 137–141.
121. Kaye SA, et al. Shiga toxin-associated hemolytic uremic syndrome: interleukin-1 β enhancement of Shiga toxin cytotoxicity toward human vascular endothelial cells *in vitro*. *Infect Immun* 1993; 61: 3886–91.
122. Kanda T, et al. Glycosphingolipid composition of primary cultured human brain microvascular endothelial cells. *J Neurosci Res* 2004; 78: 141–150.
123. Duvar S, et al. Glycosphingolipid composition of a new immortalized human cerebromicrovascular endothelial cell line. *J Neurochem* 2000; 75: 1970–1976.
124. van de Kar NCAJ, et al. Tumor necrosis factor and interleukin-1 induce expression of the verocytotoxin receptor globotriaosylceramide on human endothelial cells: implications for the pathogenesis of the hemolytic uremic syndrome. *Blood* 1992; 80: 2755–2764.
125. van de Kar NCAJ, et al. Tumor necrosis factor α induces endothelial galactosyltransferase activity and verocytotoxin receptors. Role of specific tumor necrosis factor receptors and protein kinase C. *Blood* 1995; 85: 734–743.
126. Ramegowda B, et al. Interaction of Shiga toxins with human brain microvascular endothelial cells: cytokines as sensitizing agents. *J Infect Dis* 1999; 180: 1205–1213.
127. Eisenhauer PB, et al. Tumor necrosis factor alpha increases human cerebral endothelial cell Gb₃ and sensitivity to Shiga toxin. *Infect Immun* 2001; 69: 1889–1894.
128. Stricklett PK, et al. Molecular basis for up-regulation by inflammatory cytokines of Shiga toxin 1 cytotoxicity and globotriaosylceramide expression. *J Infect Dis* 2002; 186: 976–982.
129. Ergonul Z, et al. Induction of apoptosis of human brain microvascular endothelial cells by Shiga toxin 1. *J Infect Dis* 2003; 187: 154–158.
130. O’Loughlin EV, Robins-Browne RM. Effect of Shiga-like toxins on eukaryotic cells. *Microbes Infect* 2001; 3: 493–507.
131. Müthing J. High-resolution thin-layer chromatography of gangliosides. *J Chromatogr A* 1996; 720: 3–25.
132. Müthing J. TLC in Structure and Recognition Studies of Glycosphingolipids. In: *Glycoanalysis Protocols, Methods Mol Biol*. Vol. 76 Humana Press Inc., Totowa, NJ 1998; 183–195.
133. Müthing J. TLC and HPLC of Glycosphingolipids. In: *Carbohydrate Analysis by Modern Chromatography and Electrophoresis*. J Chrom Libr. Vol. 66 Elsevier Science 2002; 423–482.
134. Müthing J, Heitmann D. Nondestructive detection of gangliosides with lipophilic fluorochromes and their employment for preparative high-performance thin-layer chromatography. *Anal Biochem* 1993; 208: 121–124.
135. Müthing J, Kemminer SE. Nondestructive detection of neutral glycosphingolipids with lipophilic anionic fluorochromes and their employment for preparative high-performance thin-layer chromatography. *Anal Biochem* 1996; 238: 195–202.
136. Meisen I, et al. Discrimination of neolacto-series gangliosides with α 2–3- and α 2–6-linked *N*-acetylneuraminic acid by nano-electrospray ionization low-energy collision-induced dissociation tandem quadrupole TOF MS. *Anal Chem* 2003; 75: 5719–5725.
137. Edgell C-JS, et al. Permanent cell line expressing human factor VIII-related antigen established by hybridization. *Proc Natl Acad Sci USA* 1983; 80: 3734–3737.
138. Stins MF, et al. Selective expression of adhesion molecules on human brain microvascular endothelial cells. *J Neuroimmunol* 1997; 76: 81–90.
139. Schweppe CH, et al. Glycosphingolipids in vascular endothelial cells: relationship of heterogeneity in Gb₃Cer/CD77 receptor expression with differential Shiga toxin 1 cytotoxicity. *Glycoconj J* 2008; 25: 291–304.
140. Levery SB. Glycosphingolipid structural analysis and glycosphingolipidomics. *Methods Enzymol* 2005; 405: 300–369.

141. Harvey DJ. Analysis of carbohydrates and glycoconjugates by matrix-assisted laser desorption/ionization mass spectrometry: An update covering the period 1999–2000. *Mass Spectrom Rev* 2006; 25: 595–662.
142. Meisen I, et al. Direct analysis of silica gel extracts from immunostained glycosphingolipids by nanoelectrospray ionization quadrupole time-of-flight mass spectrometry. *Anal Chem* 2004; 76: 2248–2255.
143. Meisen I, et al. Application of combined high-performance thin-layer chromatography immunostaining and nanoelectrospray ionisation quadrupole time-of-flight tandem mass spectrometry to the structural characterization of high- and low-affinity binding ligands of Shiga toxin 1. *Rapid Commun Mass Spectrom* 2005; 19: 3659–3665.
144. Müthing J. Analyses of glycosphingolipids by high-performance liquid chromatography. *Methods Enzymol* 2000; 312: 45–64.
145. Sandvig K, et al. Retrograde transport from the Golgi complex to the ER of both Shiga toxin and the nontoxic Shiga B-fragment is regulated by butyric acid and cAMP. *J Cell Biol* 1994; 126: 53–64.
146. Sekino T, et al. Characterization of a Shiga-toxin 1-resistant stock of vero cells. *Microbiol Immunol* 2004; 48: 377–387.
147. Dreisewerd K, et al. Analysis of gangliosides directly from thin-layer chromatography plates by infrared matrix-assisted laser desorption/ionization orthogonal time-of-flight mass spectrometry with a glycerol matrix. *Anal Chem* 2005; 77: 4098–4107.
148. Distler U, et al. Matching IR-MALDI-o-TOF mass spectrometry with the TLC overlay binding assay and its clinical application for tracing tumor-associated glycosphingolipids in hepatocellular and pancreatic cancer. *Anal Chem* 2008; 80: 1835–1846.
149. Lingwood CA. Verotoxin-binding in human renal sections. *Nephron* 1994; 66: 21–28.
150. Simons K, Ikonen E. Functional rafts in cell membranes. *Nature* 1997; 387: 569–572.
151. Brown DA, London E. Structure and function of sphingolipid- and cholesterol-rich membrane rafts. *J Biol Chem* 2000; 275: 17221–17224.
152. Anderson RGW, Jacobson K. A role for lipid shells in targeting proteins to caveolae, rafts, and other lipid domains. *Science* 2002; 296: 1821–1825.
153. Kasahara K, Sanai Y. Functional roles of glycosphingolipids in signal transduction via lipid rafts. *Glycoconj J* 2000; 17: 153–162.
154. Hoessli DC, et al. Signaling through sphingolipid microdomains of the plasma membrane: The concept of signaling platform. *Glycoconj J* 2000; 17: 191–197.
155. Cohen AW, et al. Role of caveolae and caveolins in health and disease. *Physiol Rev* 2004; 84: 1341–1379.
156. Hommelgaard AM, et al. Caveolae: stable membrane domains with a potential for internalization. *Traffic* 2005; 6: 720–724.
157. Stan RV. Structure and function of endothelial caveolae. *Microsc Res Tech* 2002; 57: 350–364.
158. Frank PG, et al. Caveolin, caveolae, and endothelial cell function. *Arterioscler Thromb Vasc Biol* 2003; 23: 1161–1168.
159. López JA, et al. Receptors, rafts, and microvesicles in thrombosis and inflammation. *J Thromb Haemost* 2005; 3: 1737–1744.
160. Nabi IR, Le PU. Caveolae/raft-dependent endocytosis. *J Cell Biol* 2003; 161: 673–677.
161. Parton RG, Richards AA. Lipid rafts and caveolae as portals for endocytosis: new insights and common mechanisms. *Traffic* 2003; 4: 724–738.
162. Kovbasnjuk O, et al. Role of lipid rafts in Shiga toxin 1 interaction with the apical surface of Caco-2 cells. *J Cell Sci* 2001; 114: 4025–4031.
163. Falguières T, et al. Targeting of Shiga toxin B-subunit to retrograde transport route in association with detergent-resistant membranes. *Mol Biol Cell* 2001; 12: 2453–2468.
164. Katagiri YU, et al. Activation of Src family kinase yes induced by Shiga toxin binding to globotriaosyl ceramide (Gb3/CD77) in low density, detergent-insoluble microdomains. *J Biol Chem* 1999; 274: 35278–35282.
165. Takenouchi H, et al. Shiga toxin binding to globotriaosyl ceramide induces intracellular signals that mediate cytoskeleton remodeling in human renal carcinoma-derived cells. *J Cell Sci* 2004; 117: 3911–3922.
166. Smith DC, et al. The association of Shiga-like toxin with detergent-resistant membranes is modulated by glucosylceramide and is an essential requirement in the endoplasmic reticulum for a cytotoxic effect. *Mol Biol Cell* 2006; 17: 1375–1387.
167. Falguières T, et al. Functionally different pools of Shiga toxin receptor, globotriaosyl ceramide, in HeLa cells. *FEBS J* 2006; 273: 5205–5218.
168. Lencer WI, Saslowsky D. Raft trafficking of AB₃ subunit bacterial toxins. *Biochim Biophys Acta* 2005; 1746: 314–321.
169. Gaus K, et al. Visualizing lipid structure and raft domains in living cells with two-photon microscopy. *Proc Natl Acad Sci USA* 2003; 100: 15554–15559.
170. Kemper B, et al. Investigation of living pancreas tumor cells by digital holographic microscopy. *J Biomed Opt* 2006; 11: 34005.
171. Müthing J, et al. Mistletoe lectin I is a sialic acid-specific lectin with strict preference to gangliosides and glycoproteins with terminal Neu5Ac α 2–6Gal β 1–4GlcNAc residues. *Biochemistry* 2004; 43: 2996–3007.
172. Gerber A, et al. Clinical course and the role of Shiga toxin-producing *Escherichia coli* infection in the hemolytic-uremic syndrome in pediatric patients, 1997–2000, in Germany and Austria: a prospective study. *J Infect Dis* 2002; 186: 493–500.
173. Banatvala N, et al. The United States national prospective hemolytic uremic syndrome study: microbiologic, serologic, clinical, and epidemiologic findings. *J Infect Dis* 2001; 183: 1063–1070.
174. Tozzi AE, et al. Shiga toxin-producing *Escherichia coli* infections associated with hemolytic uremic syndrome, Italy, 1988–2000. *Emerg Infect Dis* 2003; 9: 106–108.